ANCIENT BRONZES OF THE EASTERN EURASIAN STEPPES

from the Arthur M. Sackler Collections

EMMA C. BUNKER
with
TRUDY S. KAWAMI KATHERYN M. LINDUFF
WU EN

Published by
THE ARTHUR M. SACKLER FOUNDATION
Distributed by Harry N. Abrams, Inc., Publishers
1997

Appendix 2

Technical Studies and Metal Compositional Analyses of Bronzes of the Eastern Eurasian Steppes from the Arthur M. Sackler Collections

by W. T. Chase and J. G. Douglas

INTRODUCTION

Technical studies and metal compositional analyses of bronzes augment purely stylistic studies, aiding scholars in the formation of groups of bronzes according to origin (production areas or schools), helping in the determination of authenticity, and answering questions related to forgeries. We hope that this preliminary study will aid others in the study of bronzes from the eastern Eurasian steppes, and further the understanding of how human activity from antiquity through the present has affected the objects that remain today. This study helps us develop a cultural context for these objects, which currently exists only in the most rudimentary form.

The aim of this work is to determine fabrication methods of the bronzes, subsequent surface treatments, surface corrosion, and metallic composition. Thus we discover the raw materials used in bronze casting, suggest possible uses of the bronzes in archaeological times, record their deterioration, and recommend conservation treatment. The main approach of this work was to employ non-destructive analytical methods, which allow the objects to remain completely intact. This decision allowed the study to proceed without the necessity for sampling the objects. Primary techniques used were optical microscopy, radiography, and x-ray fluorescence. Since part of the reason for the study was to increase the accuracy and usefulness of the catalogue, some emphasis was put on resolving questions of authenticity. Four bronzes were actually sampled for a pilot study of lead-isotope ratio analysis using mass spectroscopy.

Fabrication and casting methods studied with the aid of X-radiography

The fabrication methods that had been used in making the bronzes were studied by careful observation using the unaided eye and by stereo microscopy. X-ray radiography was also used to look at fabrication methods, general condition, porosity, lead distribution, internal corrosion and the presence of breaks and repairs.

Radiography produces a permanent visible film record of the internal features of the bronze. A radiograph is produced by the passage of radiation through an object onto a film. In this case, we used high energy x-rays produced by a Gemini 320 industrial x-ray instrument at the Freer Gallery of Art. Each bronze was radiographed at 300 KV and 2 mA, as a stereo pair with 15 degrees separation on Kodak Type M and SR film.

The radiation proceeds in straight lines to the object; some of the x-rays pass through and others are absorbed—the amount transmitted depending on the nature of the material and its thickness. Darker regions on the film represent the more penetrable parts of the object, and the lighter regions, those areas more opaque to x-rays. Radiography of all of the bronzes in the catalogue was done as a part of the examination procedure. Presence of internal corrosion could be used as an indicator of authenticity. Genuinely old bronzes often seemed to have a spotty and variable lead distribution, although this was not universally true. Radiography was very helpful in revealing old repairs, so that we did not include repair metal in the compositional analyses described below.

The question of casting in a piece mold versus casting by the lost-wax method came up repeatedly in our study. In piece-mold casting, the mold is made so that it can be disassembled and the internal cavity worked on prior to casting. The mold can be built up around a model, which is then removed, or simply made off-hand. Some of the earliest piece molds were made from carved stone.

In lost-wax casting, a model of the object is made in wax or some other suitable organic material. The model (and its attached sprues and vents) are

invested in a refractory material such as clay, which is then fired. The wax runs out on melting; any remaining wax is carbonized as the temperature rises. When the molten metal is poured in, it takes the place of the wax.

Both processes leave visible traces. In piece-mold casting, the joints of the molds leave mold flash where the liquid metal runs into the crack. Finishing removes much of this mold flash, but some usually remains in crevices and often on the back of the object. Dislocations often can be seen along the mold joints. Lost-wax casting typically does not leave mold flash or evidence of mold joints. However, if the wax model is formed using a piece-mold, mold marks may be left on the wax which, in turn, are reproduced on the finished casting. These mold marks are generally softer and less visible than original mold flash from piece-mold casting. Another visible feature producing evidence of lost-wax casting is small positive round spheres that can be seen on the surface of the metal. These arise from entrapped air in the investment material, which leaves rounded cavities. When the bronze runs in, it fills the cavities and produces the spheres.

Some objects , such as LRN 2742 (No. 142, V-7092) and LRN 2643 (No. 147, V-7073), were made in piece molds and clearly show mold marks around the loops at the back, as does LRN2747 (No. 155, V-7026). All three are from the South Central Inner Mongolia group (Chapter 6, pp. 202–16), and are high-tin, moderate-lead bronzes. On the other hand, LRN 2748 (No. 199, V-7051) is a high-lead, low-tin bronze and shows the raised edges around the plaque typical of lost-wax casting. Internal corrosion can be seen on the radiograph and the surface corrosion is typical of high-lead bronzes. It is genuinely old and made in the lost-wax method.

One of the most interesting groups is the series of three plaques showing a crouching wolf devouring a doe head, LRN 2098 (No. 203, V-7022), LRN 2624 (No. F24, 72.2.450), and LRN 2640 (No. F24, V-7023). The first is an original, old, lost-wax casting with good, if thin patination. Internal corrosion can be seen on the radiograph. On the back of LRN 2098 there are three raised blobs of metal, the small spheres which signal lost-wax casting. The next, LRN2624, also shows the three raised blobs, but here they are somewhat flattened. The patina is not genuine; it dissolves in MI-2 solvent mixture. Crushed malachite (commonly used in false patination) is also visible. LRN2624 was made from LRN 2098, using a mold. LRN 2640 shows the same three blobs, even flatter, and was probably made from LRN 2624. So we have the original and two generations of reproductions represented here.

The reproduced blobs on the back of these three plaques demonstrate that the original was used as a model for the other two. The method of casting is not clear, but the copies may have been fabricated by simply coating the original with a parting agent and using plaster of Paris to mold it. If so, the mold would have to part somewhere so that the original could be removed, and in fact, on the latter two we see a mold line around the edge of the plaques. We have been calling this an "intermediate mold line", and it occurs commonly on forgeries. In bronzes with a relatively high zinc content (see analytical section below) we often find visible "intermediate mold lines", indicating that they are forgeries.

Like any criterion, however, the intermediate mold line is not infallible. Consider the twenty small stag garment ornaments in the collection of Leon Levy and Shelby White.[1] From corrosion, microscopic appearance, and radiographic appearance we have absolutely no question as to the age of these ornaments. Yet they also show the intermediate mold line, with different prominence on different plaques. In the radiographs of these pieces, the stags can be superimposed quite exactly, but the long horizontal attachment loops on the back[2] do not superimpose. Our hypothesis is that these plaques were made from a negative two-piece mold (in wood, metal, clay, or almost any material) which was filled with wax. When the mold was opened, the plaque had a line around its edge, and some mold flash (in wax) across the interior spaces in the design. The flash was pared down; traces cast in bronze can be seen on the interior spaces on some of the pieces. The horizontal attachment loops were added as two posts and a cross-bar, also in wax. Under the microscope, one can see the toolmarks that were made when the wax was carved, at the ends of the attachment loops. Then the pieces were invested and cast. Here we have twenty examples of the intermediate mold line on genuine objects.

Surface treatments

While gilding is present on a few pieces, tinning is the most prominent metal coating technique on the bronzes from the Sackler collections in this study. Some cases of stone inlay occur as well, but none with inlay of precious metals are present.

Gilded bronzes in this study were analyzed by x-ray fluorescence spectroscopy, and were found to contain

gold and a small amount of mercury. The presence of mercury strongly suggests that these objects were mercury gilded.

Differentiating intentional tinning from tin sweat (developed on high-tin bronzes during casting) can be difficult without taking a metallographic section to look at the distribution and phases comprising the tin-containing coating. In tin sweat, since the high-tin phase (the delta, 32.66% Sn) is formed inside the casting and forced to the surface during cooling, the coating will contain no more than 32.66 percent tin. If pure tin or any of the higher tin phases occur on the surface, one can immediately tell that the tin was intentionally applied.[3] X-ray fluorescence is, however, not an ideal technique for the determination of the amount of tin in a coating. The x-rays tend to penetrate the thin coating and excite fluorescent x-rays from the metal underneath it. The measured tin content has more to do with the body metal (or the extent of corrosion) than the coating. In fact, the best indicator of a tinned coating is visual recognition of it. In many cases, coatings from tinning retain their shiny, silvery-white appearance, at least in some spots.

It is very helpful if visual observation of tinned surfaces can be combined with study of the coating under the scanning electron microscope. Tinned surfaces can be clearly detected, and worn areas clearly seen to be devoid of tin, using low-energy x-rays for the detection of tin in vacuum.

In general, tinning is not very common on the Sackler bronzes; only 20 of the 156 bronzes in this study have tinned surfaces.

Corrosion

The study of corrosion on the surfaces of the bronzes was accomplished by visual examination using a stereo microscope and by testing for solubility of corrosion with solvents. Obviously, true corrosion cannot be removed with solvents. If the corrosion is painted on or enhanced by the application of paint, it will tend to be soluble to some degree. Each bronze was tested with MI-2 solvent mixture, which contains 70 percent toluene, 10 percent ethyl alcohol, 10 percent ethylene dichloride, 5 percent cellosolve and 5 percent cellosolve acetate. Most applied patinas will dissolve to some degree in this mixture. Care needs to be taken with solvent tests, as soil and other accretions can be removed and confused with applied patinas. In some cases, authentic bronzes have been touched up with pigments to disguise damage and repairs.

Painted patinas often (but not always) fluoresce in ultra-violet illumination. A UV lamp was used as a supplement to testing the patina with solvents, and did resolve some questions.

Many of the authenticated high-tin bronzes had a flat glossy tin oxide patina. Bronzes of lower tin content often had surface corrosion consisting of cuprite or tin oxide under malachite. Such corrosion is visible using the stereo microscope, and consists of a red and/or black layer underneath green. Often evidence of cleaning is visible on these bronzes, and sometimes thicker corrosion can be seen in crevices and recessed areas. Highly-leaded bronzes show a whitish corrosion, probably due to white cerrusite and hydrocerrusite; this can often be quite crystalline and sparkle like coarse sugar. Light green corrosion can also be seen on highly-leaded bronzes when the lead corrosion is mixed with copper corrosion minerals. Copper corrosion is very common on these bronzes. It is typically green in color due to the presence of malachite, and is often quite thick and coarse-grained.

The forgeries, as a group, tend to have thinner patinas. Glossy brown or black patinas were seen, along with matte black and black with thin red layers. These patinas were not tested for composition, since that would have required removing a sample. Some of them, however, look like applied sulfide patinas. In two cases we noted that applied patinas seemed to contain textile impressions. These are noted in the individual entries in Appendix 3. Further investigation of the applied patinas on these objects should prove rewarding.

It should, however, be pointed out that even if a bronze is covered with a totally false patina, it does not prove that it is a forgery or a later production. It could have been stripped of its original patina and then repatinated to make it more saleable. There are well-known instances where ancient bronzes were partially cleaned, then the cleaning stopped and the patina restored in the cleaned area. Other bronzes have been repatinated to improve their appearance, and a few cases are known where vessels with a shiny, dark patina have been turned matte green to increase salability.[4] If one can take a cross-section to see how the corrosion penetrates into the metal, one can be much surer of the age of the bronze. Compositional analysis also helps in determining whether a bronze is genuine.

Compositional Analysis:

Analytical considerations

X-ray fluorescence spectrometry (XRF) was chosen for the analysis of the eastern Eurasian steppes bronzes primarily because it is a technique which allows the determination of major and minor elemental compositions of metal in a rapid, non-destructive manner, without sampling. We used an OMEGA FIVE x-ray fluorescence spectrometer, which is a modified Spectrace Model 6000. This instrument includes an open x-ray beam architecture for analysis of large objects without the need for sampling and/or analysis in a vacuum chamber. This is possible because its Si(Li) detector is electrically-cooled. Unlike the bulkier liquid nitrogen-cooled detectors, an electrically-cooled detector can be mounted on a moveable turret and positioned to analyze the surface of a wide range of 3-dimensional objects. X-ray beam positioning is accomplished using a double beam Helium-Neon laser alignment system. The instrument has a 50 KV, 1.0 mA rhodium target x-ray tube. It has three x-ray filter positions: unfiltered, thin rhodium and aluminum. The x-ray beam can be collimated with three apertures: 1 mm, 2.5 mm, and 5 mm.

X-ray fluorescence analysis with the OMEGA FIVE is carried out in an atmosphere of air which precludes the detection of elements with atomic number less than that for argon (atomic no. 18); air attenuates the lower-energy x-rays.

X-ray fluorescence is a surface technique which includes a much larger analyzed area than many techniques that require sampling such as scanning electron microscopy, electron microprobe, x-ray diffraction and Fourier-transform infrared spectroscopy. As mentioned above, the x-ray beam can be collimated with three apertures. The approximate diameters of the analyzed oval-shaped areas achieved using these apertures are: 0.5 cm, 2.0 cm and 3.3 cm. In practice, the largest aperture possible is used, which provides the most x-ray signal at the detector.

The x-ray fluorescence conditions used for bronzes from the eastern steppes were 45 KV, 0.99 mA, a thin rhodium filter and 100 seconds live time. The medium collimator was used which allows an analysis of an oval-shaped area with a diameter of approximately 2.0 cm. In some cases, the small collimator was used with an analysis area with a diameter of approximately 0.5 cm. The quantitative program used is the Fundamental Parameters Program (Version 1.34a) provided by Spectrace, Inc. Metal standards used in this quantitative XRF procedure are shown in Table 1.

At least two XRF analyses were performed on different spots on each object. In Table 2 the analytical result set which was determined to best represent the bulk composition of the object is reported. In many cases, this is the analytical result set with the lowest lead obtained in the two or three (or more) XRF determinations.

Leads tend to be higher than they should be, and the results with the lowest lead often seemed to reflect most accurately the bulk composition of the metal (see the further lead discussion below).[5] Where possible, the area analyzed was that previously cleaned by milling for earlier analytical studies by Samolin and Drew (1965) or by Drew (1971).

Since XRF is a surface technique, there are inherent problems in using this method on corroded bronzes which have presumably been buried. Any alteration, contamination, corrosion or applied material on the surface of a metal object will be included in the analysis. A flat, clean, polished surface gives the most reliable XRF analysis. Because the surfaces of these bronzes are often not flat, precision and accuracy may be compromised. In cases where higher precision and accuracy are needed, other techniques should be used such as inductively-coupled plasma or atomic absorption spectrophotometry. XRF, however, is a useful tool for answering many archaeological and art historical questions in a nondestructive manner.

The problems are particularly severe in the case of lead. In higher percentages (5% and above) lead segregates severely in casting. In addition, it is often the first alloy constituent to corrode. This means either that it may be decreased in the analyzed area due to dealloying, or, more commonly, that an increased lead signal may result from layers of lead corrosion on the surface. Lead can also smear across the surface in polishing. And, since lead exhibits such a high x-ray absorption, it will distort the analysis even if only a very thin film is present on the surface.

Another problem associated with lead determinations using XRF is the lack of bronze standards with as high a lead content as the ancient bronzes. Such standards are not available commercially to the best

of our knowledge. As shown in Table 1, the highest lead value given is for the Tyseley GC-9 standard, with a lead composition of 11.60 percent. This means that our lead determinations are reasonable up to this amount, but for highly-leaded bronzes, especially 20 percent or higher, lead determinations by XRF are simply not reliable. The exact quantities of lead in highly-leaded bronzes should be determined by another analytical method. An associated problem with the analysis of highly-leaded bronzes is that extraordinarily high lead values may affect the relative amounts of the other elements detected. Atil, Jett and Chase[6] give an example which shows just how different from the actual contents x-ray fluorescence surface analyses can be. In their study, two Freer bronzes were chosen for comparison. Both had previously been analyzed by wet chemistry. The first had a lead content of 1.4 percent by wet chemistry which is in good agreement with a lead content of 2.2 percent by x-ray fluorescence. The second had 16.6 percent lead by wet chemistry (with a confidence limit of +-0.2) and 22 percent by XRF (C.L.+-14%). While the difference in the means of the analyses is not too large, the range in the XRF values is huge (30.7%, 15.5%, 13.9%, and 29.0%). Lead analyses above 10 percent or so determined by XRF should be considered only an indication that the object has a high lead content and should not be used quantitatively.

A similar problem exists with the analysis of arsenic. The highest arsenic value used in the quantitative procedure was 3.5 percent arsenic in the HL3.5 percent standard, supplied to us by Heather Lechtman of MIT. Arsenical bronze standards are not, as far as we know, commercially available. Quantitative XRF data is probably unreliable at arsenic values above 3.5 percent due to lack of appropriate standards. Tin, copper, and iron should be more easily quantified, but with the uncertainty in the lead and arsenic coupled with the fact that the procedures normalize the results to 100 percent, one must use the results obtained with care.

Analytical results

Compositional data for the authenticated bronzes and forgeries are given in Table 2. These analyses represent a relatively small body of data, given the vast range in geographical and chronological origins of these materials. Nevertheless, several trends are starting to emerge. The most interesting metal components are tin, lead, arsenic and zinc.

Authenticated bronzes from the Sackler Collections

Both tin and lead are present in widely varying amounts in the authenticated bronzes. Lead-, tin-, and lead-tin bronzes are represented throughout the bronze objects from various geographic and chronological ranges. Several phenomena may account for this seemingly random distribution. As mentioned above, lead analysis by XRF represents an challenge especially in the highly-leaded bronzes. Such analyses may not be correct, and may skew relative compositions of the other alloying elements. Problems also arise with the tin analysis by XRF when bronzes have been tinned, or due to surface enrichment of tin by corrosion.

Some general trends, however, can be seen in tin and lead compositions. The earlier bronzes from Mongolia and Southern Siberia (Chapter 3) are higher in tin, ranging from 10.8 to 24 percent. Later bronzes from this area (Chapter 8B) show lower tin contents, ranging from 0.12 to 6.4. Bronzes from Northern Hebei and South Central Inner Mongolia (Chapter 6) contain high tin contents, ranging from 13.4 to 30 percent. Inferences on particular alloy compositions used for these bronzes will have to await a more extensive study, given the wide range of tin and lead contents of all of these bronzes, and the relatively small number of bronzes analyzed.

Bronzes from Mongolia and Southern Siberia in both the earlier and later time periods (Chapters 3 and 8B) contain significant amounts of arsenic. The three Xianbei bronzes from Northeastern China also contain significant amounts of arsenic. As mentioned above, the analysis of arsenic in amounts higher than 3.5 percent is difficult due to the lack of metal standards with arsenic contents above this amount. However, the presence of arsenic in relatively high amounts can help verify that bronzes in which this occurs may originate in Siberia. It is interesting that the highest arsenic bronze in our group, No. 241, V-7052 (LRN2101) with an arsenic content of 12.1 percent, iron content of 4 percent, and a zinc content of 0.17 percent is very similar in shape to two plaques from a Xiongnu cemetery at Derestuy; one of these excavated plaques also has 1.4 percent zinc. Variability of alloys seems to be a general characteristic of bronzes from the eastern Eurasian steppes.

Other authenticated bronzes generally have low arsenic contents of 0.00 to 0.50 percent rather like contemporaneous Chinese bronzes. These low arsenic contents indicate that arsenic was not inten-

tionally added as an alloying component. More likely, low levels of arsenic were introduced along with other major alloying components such as copper.

Forgeries from the Sackler Collections

The wide range in metal compositions among the forgeries is not surprising considering that these bronzes where probably made over a long time and a broad geographical range. Incidentally, the small bronze stamp seals also known as "Nestorian crosses" (see Appendix 5) would be very interesting to compare in terms of material with the Eurasian steppe bronzes.

A couple of interesting elemental trends were noted within the forgeries category. First, many of these forgeries contain significant amounts of zinc. Bronzes with a relatively high zinc content (above approximately 0.75%), could arguably contain this element as an alloying component. It does seem to occur in amounts of up to 1.5 percent in bronzes that one could consider authentic from periods contemporary with Eastern Zhou onwards in the Far East (see the Xiongnu plaque from Derestuy above, and our laboratory records on belt hooks in the Freer Gallery.) Much higher contents of zinc indicates a brass alloy. This content allows the bronzes to be attributed to a more recent date, as brasses alloyed with metallic zinc were not commonly produced until the late-17th century. Traces of zinc are often present in bronzes made today, and zinc traces may serve to indicate the possibility that the piece is not authentic.

Another elemental trend seen in the forgery category is elevated amounts of lead. This is not surprising as lead has always been a cheaper metal additive.[7] It also makes the metal easier to cast and to finish, and can aid in the development of a nice, dark artificial patina.

Previous compositional analyses of this collection at Columbia University

Previous analysis of some of the bronzes in this catalogue, along with others in the Sackler collections, were done by Samolin and Drew (1965), and Drew (1971) using optical emission spectroscopy. Data from these studies are shown in Table 3, and combined with our data in Table 4 and Figures 1–8.

Discrepancies were found in the analysis of some objects in this study using XRF and Samolin and Drew (1965), and Drew (1971) using optical emission spectroscopy. Twenty-three objects were analyzed by both analytical techniques. The analyses of these objects are in general agreement; some exceptions are No. 218 (V-7074), No. 223 (V-7008), No. 224 (V-7015) and No. 240 (V-7021). Samolin and Drew (1965) found less lead by optical emission spectroscopy than the present study by XRF. This difference may be partially to the difference in analytical technique (emission spectrography is notorious for underestimating high lead contents), and more importantly, due to the inherent problems with the analysis of lead using XRF discussed above. Arsenic amounts also tend to be different. The results are, however, similar enough to warrant combining them for the general statistics below.

General trends in zinc, lead, and tin

All of the analyses of this collection that are available to us are shown in Table 4 and Figures 1–4. Histograms for zinc and lead contents in genuine Eurasian steppe bronzes and forgeries illustrate that the authentic bronzes tend to have much less zinc and also less lead than the forgeries.

Zinc is of particular interest for detecting forgeries. To reinforce this idea, we show in Table 4 all of the bronze analyses in order of decreasing zinc content. The first bronze that we consider to be authentic which one encounters in this table is No. 249 (V-7198, LRN2754) a Xianbei bronze with moderate lead and high arsenic. It could well be that the polymetallic ores which were used for these bronzes contained both zinc and arsenic; multivariate analysis on this data would be a productive field for future research. While it is difficult to illustrate trends in compositions for the authentic Eurasian steppe bronze groups chapter by chapter for the catalogue, some comparisons of authentic bronzes and forgeries are very helpful. Figure 5, a plot of lead versus tin for authentic bronzes, shows a random distribution. There is some clustering of values in the low lead area. Figure 6 shows a similar lead versus tin plot that includes forgeries as well. All the data points for the forgeries lie in the lower half of the diagram. They are generally higher in lead and lower in tin than the authentic Eurasian steppe bronzes.

In an attempt to make more sense out of these distributions, we determined correlation coefficients for the various elements in the Eurasian steppe bronzes. The two most significant correlation coefficients were copper and lead (-0.878) and copper and tin (-.470). This shows that high copper is correlated with low lead. In fact, if one plots lead versus copper (Figure 7) the relationship is abundantly clear. It is, however,

of great interest that the lead-copper distribution for the forgeries (the black squares) is much tighter than that for the authentic pieces. The converse is true for tin (Figure 8). Here the authentic pieces have a much tighter and higher distribution, suggesting that the bronze formulation for the authentic pieces is being made in terms of copper and tin, and some lead being thrown in at random. Forgeries, however, are being made by the addition of lead to copper, with some tin thrown in. This agrees with what we have inferred about ancient alloying practice,[8] and it is interesting to see such a clear difference between these two distributions.

Lead isotope ratio measurements

Samples were taken from four plaques, two published in this catalogue, and two which are not included. One of the latter is from the Calon da collection. Lead isotope analysis was performed by thermal ionization mass spectrometry by Emile Joel of the Smithsonian's Conservation-Analytical Laboratory.[9] The results are shown in Table 5 and Figure 9. One of the plaques, No. F8 (V-7107) is believed to be a forgery because of its high lead content and corrosion-free appearance. While lead isotope ratio analysis does not prove that this piece is late, it does fall in an area of the lead isotope diagram with relatively few other objects. One object with lead isotope ratios similar to V-7107, is an elongated late belt hook in the Freer collection (F19.69A). This work has been assembled by soldering rather than by casting. One of the two longest belt hooks in the Freer collection—the other is F16.441, another late example—contains zinc, as does the second hook. The forgeries and late pieces in our lead isotope ratio data base do not cluster. They do not seem to form groups, and No. F8 (V-7107) is yet another isolated example of a forgery.

A small S-shaped plaque, V-7155, like No. 141 falls between the example mentioned above and the group formed by the two other plaques. We do not yet have an elemental analysis of V-7155. Some of the leads published by Kon'kova[10] fall in a similar area of the diagram. The lead for V-7155, an unpublished work, is not near any of the Han mirror groups (see below).[11] Perhaps this is lead from a Siberian source.

The other two plaques, No. 224 (V-7015) and LTS 1994.4.16.1 (LRN2152), the Calon da plaque, fall at the upper corner of the distribution and are quite close to each other. The first has been placed in Chapter 8A, "Northern China." No. 224 (V-7015) contains no arsenic; the metal composition looks like a typical late-Zhou Chinese alloy. The second is very similar to a set excavated at Maoqinggou.[12] Many more determinations would be necessary to make judgements based on lead isotope ratios, but this pilot study has shown that there are both differences and groupings within the Eurasian steppe material. It forms an interesting field for future research. We would like to thank Emile Joel for performing the analyses and the National Institute for Standards and Technology for making facilities available.

CONCLUSION

The development of metallurgy in the Eurasian steppe region is extremely complex and varied as dictated by the expanse of its geographical region and long history. The challenges of learning about this area of archeaometallurgy is compounded by the number of forgeries and other copies of these bronzes that have been made. Although the present interpretation of the data presented in this study is preliminary, we hope that it will help scholars in future study of these and related materials.

1. So & Bunker 1995, p. 160, no. 83.
2. So & Bunker 1995, p. 160 detail.
3. Meeks 1986; Han & Bunker 1993.
4. Gettens 1969, p. 226.
5. Atil, Chase & Jett 1985, p. 263.
6. 1985, pp. 262–64.
7. Chase 1983.
8. Chase 1983.
9. Chase, Barnes & Joel 1995.
10. Kon'kova 1990.
11. Mabuchi, Hirao & Nishida 1985.
12. So & Bunker 1995, p. 192, no. 86a.

Table 1. Copper alloy standards used in the quantitative XRF procedure.

	Cu	Zn	Pb	Fe	Sn	As
1. GC-1[A]	91.44	—	0.60	—	7.86	—
2. GC-9[A]	80.96	—	11.60	—	7.94	—
3. BE-2[A]	84.8	14.6	—	0.56	—	—
4. BE-6[A]	65.1	32.8	—	2.13	—	—
5. OLIN544-2[B]	89.3	2.4	4.1	—	4.0	—
6. HL-1%AS[C]	98.9	—	—	—	—	1.01
7. HL3.5%AS[C]	96.5	—	—	—	—	3.52
8. BRAM323[D]	84.85	—	0.20	—	14.75	—

Sources of these standards are as follows:
A = Tyseley Copper Alloy Standards;
B = Olin-Matheson Alloy Standards;
C = Copper–Arsenic standards prepared by Heather Lechtman, Massachusetts Institute of Technology (Feb. 1985), composition determined by Atomic Absorption Spectrophotometry, Janet G. Douglas (1986);
D = Brammer Copper Alloy Standards.
Note that a dash (—) indicates that no value was used in the XRF quantitative procedure.

Table 2. Metallic composition of selected bronzes from the eastern Eurasian steppes determined by X-ray fluorescence spectroscopy (XRF).

(Items presented in the tables are in catalogue order by accession number.)

Acc No	LRN[1]	Cu	Sn	Pb	As	Fe	Zn
Chapter 1. The Bronze Age in Northwestern China							
V-2029	2862	77	20	2.9	0.00	0.26	0.14
V-2031	2863	69	24	6.7	0.00	0.20	0.00
V-3377	2866	89	9.5	1.00	0.00	0.44	0.00
V-2028	2861	84	0.21	4.4	11.1	0.42	0.00
Chapter 3. The Bronze Age of the Far North							
V-3100	2864	76	24	0.13	0.27	0.99	0.12
V-3312	2865	59	28	6.19	6.1	0.47	0.01
V-3449	2867	78	20	1.12	0.75	0.13	0.00
V-7302	2791	88	10.8	0.05	0.08	0.58	0.00
Chapter 4. The Iron Age in Northeastern China							
V-3057	2657	78	6.8	14.3	0.40	0.25	0.00
Chapter 5. The Iron Age in Northern Hebei							
V-7315	2868	78	15.7	5.6	0.00	0.10	0.00
V-7077	2750	65	17.5	16.8	0.00	0.15	0.20
V-3538	2615	47	28	24	0.00	0.19	0.50
Chapter 6. The Iron Age in South Central Inner Mongolia							
V-7325	2105	85	13.4	0.60	0.13	0.29	0.14
V-7092	2742	64	30	5.8	0.00	0.25	0.00
V-7073	2643	75	22	2.2	0.19	0.19	0.13
V-7026	2747	89	16.4	2.6	0.00	0.07	0.20
Chapter 7A. Northwestern China and Southwestern Inner Mongolia							
V-3428	785	68	11.5	20	0.00	0.36	0.03
Chapter 7B. The Iron Age in Northwestern China: Ningxia & Gansu							
V-7051	2748	82	1.6	15.6	0.00	0.51	0.07
72.2.448	0189	75	4.0	21	0.00	0.13	0.00
V-7194	2789	68	11.2	20.0	0.00	0.45	0.00
V-7022	2098	87	5.0	7.7	0.07	0.18	0.15
Chapter 8A. The Xiongnu Period in Northern China							
V-7074	2749	70	7.3	22	0.00	0.49	0.15
72.2.443	2655	78	2.1	19.9	0.00	0.17	0.01
V-7008	2092	66	6.8	25	0.68	1.1	0.28
V-7015	2094	71	13.5	13	0.00	1.7	0.43
V-7009	2745	51	10.1	38	0.00	0.35	0.25
V-7000	2743	95	0.57	1.3	0.06	2.8	0.04
V-7015	2094	71	13.5	13	0.00	1.7	0.43
Chapter 8B. The Xiongnu Period in Mongolia, Buryatia & S. Siberia							
72.2.442	2622	83	0.24	8.8	7.8	0.14	0.14
V-7148	2618	86	1.7	0.30	10.7	1.2	0.14
V-7024	2099	98	0.44	0.09	0.32	1.3	0.13
V-7021	2097	91	3.5	3.4	1.20	0.43	0.20
V-7052	2101	80	3.0	1.17	12.1	4.0	0.17
V-3925	2787	69	6.4	22	1.8	0.24	0.14
V-7013	2093	92	1.36	3.6	2.3	0.19	0.33
V-3032	2784	95	0.12	0.82	3.1	1.03	0.00
Chapter 9. Xianbei Artifacts from the Northern Zone							
V-7198	2754	95	0.39	1.37	1.80	0.87	0.56
V-7147	2103	60	10.1	30	0.59	0.00	0.16
V-7050	2100	89	3.2	7.2	0.66	0.18	0.00
Chapter 10. The Eastern Eurasian Steppes							
V-3103	2628	87	10.8	1.36	0.21	0.82	0.17
V-3475	2775	91	1.7	3.10	0.07	4.4	0.00
V-7062	2788	72	4.1	22	0.43	0.85	0.01
V-7061	2617	71	12.8	13.9	0.39	1.6	0.01
V-7185	2648	86	6.8	6.9	0.13	0.00	0.03
V-3315	2631	84	10.4	5.8	0.27	0.00	0.06
Appendix 3. Northern Zone Forgeries							
72.2.19	2621	87	10.5	2.0	0.09	0.00	0.26
V-7346	2651	76	7.9	15.5	0.28	0.00	0.12
72.2.29	2613	72	0.89	15.9	1.6	0.00	9.29
V-3089	2626	79	6.3	9.6	0.80	4.4	0.27
V-3176	2629	79	6.5	13.3	0.41	0.00	1.2
V-3514	2089	47	5.8	45	1.2	0.00	0.50
V-3079	2656	78	7.5	12.5	0.42	0.92	0.35
V-7107	2150	58	13.2	27	2.2	0.00	0.10
V-7277	2619	64	6.9	26	0.68	0.32	.8
V-7012	2638	98	0.26	1.4	0.21	0.03	0.06
V-7076	2644	79	5.4	15.1	0.36	0.00	0.56
V-4560	2635	69	4.5	26	0.50	0.00	0.36
V-7053	2641	70	4.1	21	1.3	0.37	3.1
V-3462	2652	78	2.3	5.9	5.6	1.2	7.5
V-3588	2653	85	4.7	9.9	0.19	0.27	0.37
V-7174	2647	70	3.8	9.4	13.4	0.50	2.7
72.2.107	2620	67	4.2	24	1.6	0.00	3.7
72.2.456	2625	90	0.89	2.6	0.5	0.29	5.6
V-7016	2095	69	10.5	20	0.67	0.00	0.30
V-7184	2776	68	14.0	17.5	0.17	0.00	0.56
V-3102	2627base	86	11.1	1.2	0.21	1.04	0.13
V-3102	2627bull	79	1.1	9.1	2.0	4.4	4.7
V-7007a	2636	87	4.1	7.7	0.28	0.12	0.81
V-7007b	2637	74	3.9	20.0	0.19	1.8	0.17
72.2.450	2624	77	4.1	16.7	0.86	0.00	1.1
V-7023	2640	79	6.0	12.8	0.34	0.00	1.9
V-7060	2642	94	0.39	0.56	0.23	0.47	4.3
V-3545	2634	34	10.3	42	9.0	2.5	2.0
V-7017	2096	68	6.3	16.2	2.5	6.3	0.83
V-7102	2751	40	8.5	49	1.5	0.00	0.92
72.2.445	2623	87	3.6	4.1	0.84	0.00	4.1
V-7014	2616	68	1.7	29	0.20	0.90	0.05
V-7018	2639	90	0.67	0.86	0.18	8.3	0.15
72.2.444	2085	64	1.4	6.7	2.5	0.52	25

1. Lab Record Number, Department of Conservation & Scientific Research, FGA/AMSG

Table 3. Metallic composition of selected bronzes from the eastern Eurasian steppes in this catalogue as determined by emission spectroscopy in past studies.

Acc No	Other No[2]	Cu	Sn	Pb	As	Fe	Zn
Chapter 1. The Bronze Age in Northwestern China*							
V-7343	O-1002	80-85	4.2	10-15	0.05	0.02	0.1
Chapter 2. The Bronze Age in Northeastern China*							
V-3375	O-855	85-90	9.6	1-5	0.005	0.08	0.02
V-7366	O-1038	89-91	6.7	2.6	0.2	0.001	0
Chapter 3. The Bronze Age of the Far North*							
V-7345	O-1004	96-98	2	0.45	0.8	0.007	0
V-3038	O-87	96-98	0.4	0.15	2	0.3	0
V-3040	O-88	96-98	0.004	0.01	3	0.007	0
V-7334	O-993	87-92	5.8	0	1.5	1-5	0
V-7302	O-957	93-95	5.9	0.05	0	0.4	0
V-7269	O-924	93-95	6.4	0.17	0	0.08	0

2. Numbers with O-prefix are identification numbers used in Drew 1971. Plate numbers indicate illustrations in Samolin & Drew 1965.

* Drew 1971

† Samolin & Drew 1965

Acc No	Other No[2]	Cu	Sn	Pb	As	Fe	Zn
V-7297	O-952	94-96	4.8	0.25	0.02	0.07	0.02
V-7279	O-934	90-93	5	1.3	1-3	0.01	0
V-7255	O-910	80-90	10-15	0.36	1-3	0.006	0
V-7229	O-878	96-98	0.3	0.12	2-4	0.04	0
V-7228	O-877	91-94	4.5	0.04	2-4	0.02	0
V-7217	O-865	95-98	3	0.35	0.6	0.01	0
V-7295	O-950	95-98	1.3	0.1	1-3	0.05	0
V-7230	O-879	91-93	6.	0.03	0.75	0.002	0
V-7338	O-997	97-98	0.5	0.08	3	0.01	0
V-7225	O-874	93-97	3.5	0.04	0.5	0.02	0
V-7363	O-1035	92-96	3.2	0.16	2-4	0.006	0
V-7365	O-1037	85-95	10-15	0.05	0.5-1	0.1	0
V-7432	O-31	92-96	2.5	0.14	1-3	0.04	0
V-7241	O-894	80-90	10-15	0.35	3-5	0.1	0
Chapter 4. The Iron Age in Northeastern China†							
V-7093	O-717	79	11.4	7.4	0.13	0.023	0
Chapter 4. The Iron Age in Northeastern China*							
V-7367	O-1039	83-87	7	8-10	0.05	0.04	0
V-7291	O-946	80-90	0.01	10-20	0	0	0
V-7311	O-966	75-85	10-15	5-10	0.11	0.005	0
V-7244	O-897	88-92	5.6	5.1	0.09	0.04	0
V-7220	O-869	88-92	5.5	5.1	0.25	0.02	0
V-7242	O-895	70-80	10-15	10-15	0.15	0.02	0
V-7313	O-968	75-85	5-10	10-15	0.1	0.07	0
V-7266	O-921	87-92	6-10	1	0.1	0.1	0
V-7254	O-908	85-90	4.9	5-10	0.25	0.005	0
Chapter 5. The Iron Age in Northern Hebei†							
V-7105	pl. 15:C	88	7.4	2.7	0	0	0
V-7200	pl. 15:A	89	4.2	2.5	0.13	0	0
V-3555	pl. 15:D	83	5.5	10.5	0	0.035	0
V-7106	pl. 14:A	81	14	2.6	0	0.26	0.01
V-7108	pl. 14:E	86	7.5	3.8	0	0.01	0.01
V-7046	pl. 14:D	90	1.8	4.8	0.1	0.023	0.01
Chapter 5. The Iron Age in Northern Hebei*							
V-7261	O-916	87-90	5.6	5	0.25	0.003	0
V-7260	O-915	85-90	4.5	5-10	0.03	0.004	0
V-7430	O-900	88-91	4.9	5	0.3	0.004	0
V-7268	O-923	84-88	6.9	6.8	0.04	0.01	0
V-7287	O-942	85-90	8-10	3	0.1	0.02	0
Chapter 6. The Iron Age in South Central Inner Mongolia†							
V-7026	pl. 12:A	86.9	8.3	1.98	0.47	0.042	0
Chapter 7B. The Iron Age in Northwestern: Ningxia & Gansu†							
V-7022	pl. 4:A	83.8	9.2	5.9	0.12	0.0001	0
Chapter 8A. The Xiongnu Period in Northern China†							
V-7074	pl. 17:A	83	9	6.2	0.5	0.09	0
V-7075	pl. 17:B	83	10.8	3.8	0.58	0.11	0
V-7045	pl. 17:C	75	12.7	10.4	0.7	0.065	0
V-7008	pl. 10:A	88.1	3.2	8.26	0.2	0.24	0
V-7015	pl. 6:C	89.7	7.4	0.42	0.011	0.14	0
V-7011	pl. 6:B	91.8	3.8	1.6	0.01	0.0001	0
V-7115	pl. 17:D	94	4.3	0.6	0	0.1	0
V-7009	pl. 7:A	78.8	7.8	10.4	0.42	0.11	0
V-7010	pl. 7:B	90.2	4.4	3.6	0.34	0.0005	0.001
V-7005	pl. 5:B	89.1	8.3	0.29	0.11	0.0001	0
V-7000	pl. 10:C	95.6	0.14	0.46	0	0.35	0
Chapter 8B. The Xiongnu Period in Mongolia, Buryatia & S. Siberia†							
V-7025	pl. 11:A	89.1	4.7	6.07	0	0.0043	0
V-7024	pl. 8:B	95.8	0.32	0.29	0.075	0.27	0.035
V-7021	pl. 7:C	82.2	4	5	0.36	0.085	0
V-7013	pl. 9:B	93.9	0.47	4.04	0.36	0.0001	0
Chapter 9. Xianbei Artifacts from the Northern Zone†							
V-7198	pl. 1 E	98	0.1	0.4	0.51	0.085	0
V-7048	pl. 8:C	88.8	3.6	0.074	0.22	0.17	0.03
Appendix 3. Northern Zone Forgeries*							
V-7107	pl. 16B	83	9.5	3.1	0.02	0	0.01
V-7012	pl. 5A	96.3	0.005	0.2	0.0037	0	0
V-7016	pl. 4C	85.1	7.2	6	0.0001	0	0
V-7007a	pl. 36A	80	7.2	13.1	0.26	0.48	0.13
V-7007b	pl. 36B	80	6.4	13.3	0	0.42	0.11
V-7023	pl. 4B	72.1	8.8	17.4	0.14	0.1	1.3
V-7017	pl. 8A	83.3	5.4	11.6	0.06	0.41	0.41
V-7004	pl. 13A	78.4	6.2	10.2	0.11	0.36	4.1
V-7003	pl. 13B	77.8	4.8	10.2	0.23	0.82	4.8
V-7014	pl. 9A	92.6	0.36	6.74	0.0012	0.16	0
V-7027	pl. 12C	83.5	0.38	8.74	0.27	0.09	6.5
V-7001	pl. 12B	83.8	1.8	8.62	0.059	0.15	4.6
V-7006	pl. 5C	93.4	2.4	0.39	0.18	0.01	1.4
V-7018	pl. 11B	89.2	0.37	1.97	0.0024	0.98	0

2. Numbers with O-prefix are identification numbers used in Drew 1971. Plate numbers indicate illustrations in Samolin & Drew 1965.

* Drew 1971

† Samolin & Drew 1965

Table 4. Analyses of bronzes from the eastern Eurasian steppes in order of decreasing zinc content. The zinc, lead, and arsenic figures have been rounded to two beyond the decimal.

Cat No	Acc No	Chapt No	Zn	Pb	As	Analyst‡
F35	72.2.444	App 3	25.30	6.73	2.49	1
F3	72.2.29	App 3	9.29	15.90	1.65	1
F15	V-3462	App 3	7.46	5.85	5.63	1
F32	V-7027	App 3	6.50	8.74	0.27	2
F19	72.2.456	App 3	5.63	2.60	0.48	2
F28	V-7003	App 3	4.80	10.20	0.23	2
F22	V-3102	App 3	4.73	9.11	2.00	2
F13	V-7001	App 3	4.60	8.62	0.06	2
F25	V-7060	App 3	4.31	0.56	0.23	2
F30	72.2.445	App 3	4.14	4.14	0.84	1
F28	V-7004	App 3	4.10	10.20	0.11	2
F18	72.2.107	App 3	3.70	23.47	1.64	2
F14	V-7053	App 3	3.10	20.60	1.39	1
F17	V-7174	App 3	2.65	9.40	13.49	1
F17a	V-7166	App 3	2.37	2.09	1.61	1
F26	V-3545	App 3	1.95	42.46	8.97	1
F24	V-7023	App 3	1.90	12.77	0.34	1
F9	V-7277	App 3	1.84	26.43	0.68	1
F33	V-7006	App 3	1.40	0.39	0.18	2
F24	V-7023	App 3	1.30	17.40	0.14	1
F5	V-3176	App 3	1.24	13.25	0.41	2
F24	72.2.450	App 3	1.07	16.68	0.86	1
F29	V-7102	App 3	0.92	49.18	1.51	1
F27	V-7017	App 3	0.83	16.20	2.51	1
F23	V-7007a	App 3	0.81	7.67	0.28	1
F21	V-7184	App 3	0.56	17.47	0.17	1
249	V-7198	9	0.56	1.37	1.80	1
F12	V-7076	App 3	0.56	15.09	0.36	1
132	V-3538	5	0.50	24.15	0.00	1
F6	V-3514	App 3	0.50	45.03	1.16	1
224	V-7015	8A	0.43	13.02	0.00	2
F27	V-7017	App 3	0.41	11.60	0.06	2
F15	V-3588	App 3	0.37	9.91	0.19	2
F13	V-4560	App 3	0.36	25.94	0.50	1
F7	V-3079	App 3	0.35	12.46	0.42	1
243	V-7013	8B	0.33	3.57	2.27	1

‡ Analyst: 1 = Chase & Douglas, this study.
2 = Samolin & Drew, 1965.
3 = Drew, 1971.

Cat No	Acc No	Chapt No	Zn	Pb	As	Analyst[1]
F20	V-7016	App 3	0.30	19.65	0.67	1
223	V-7008	8A	0.28	24.92	0.68	1
F4	V-3089	App 3	0.27	9.65	0.80	1
F1	72.2.19	App 3	0.26	2.03	0.09	1
231	V-7009	8A	0.25	38.10	0.00	1
112	V-7077	5	0.20	16.75	0.00	1
155	V-7026	6	0.20	2.59	0.00	1
240	V-7021	8B	0.20	3.36	1.20	1
241	V-7052	8B	0.17	1.17	12.11	1
252	V-3103	10	0.17	1.36	0.21	1
F23	V-7007b	App 3	0.17	19.97	0.19	1
250	V-7147	9	0.16	29.28	0.59	1
218	V-7074	8A	0.15	22.33	0.00	1
F34	V-7018	App 3	0.15	0.86	0.18	1
203	V-7022	7B	0.15	7.72	0.07	1
5	V-2029	1	0.15	2.94	0.00	1
238	72.2.442	8B	0.14	8.79	7.82	1
242	V-3925	8B	0.14	21.98	1.79	1
238	V-7148	8B	0.14	0.30	10.72	1
239	V-7024	8B	0.13	0.09	0.32	1
F22	V-3102	App 3	0.13	1.17	0.21	1
F23	V-7007a	App 3	0.13	13.10	0.26	2
147	V-7073	6	0.13	2.19	0.19	2
32	V-3100	3	0.12	0.13	0.27	1
F3	V-7346	App 3	0.12	15.48	0.28	1
F23	V-7007b	App 3	0.11	13.30	0.00	2
F8	V-7107	App 3	0.10	26.62	2.15	2
8	V-7343	1	0.10	12.50	0.05	3
199	V-7051	7B	0.08	15.61	0.00	1
F10	V-7012	App 3	0.06	1.36	0.21	1
263	V-3315	10	0.06	5.80	0.27	1
F31	V-7014	App 3	0.05	29.13	0.20	1
233	V-7000	8A	0.04	1.28	0.06	1
239	V-7024	8B	0.04	0.29	0.08	2
179	V-3428	7A	0.03	20.11	0.00	2
251	V-7048	9	0.03	0.07	0.22	2
262	V-7185	10	0.03	6.93	0.13	2
19	V-3375	2	0.02	3.50	0.01	3
36	V-7297	3	0.02	0.25	0.02	3
32	V-3312	3	0.01	6.19	6.06	3
132	V-7106	5	0.01	2.60	0.00	3
134	V-7108	5	0.01	3.80	0.00	2
134	V-7046	5	0.01	4.80	0.10	2
261	V-7061	10	0.01	13.92	0.39	2
F8	V-7107	App 3	0.01	3.10	0.02	2
220	72.2.443	8A	0.01	19.94	0.00	2
260	V-7062	10	0.01	22.49	0.43	1
231	V-7010	8A	0.00	3.60	0.34	2
5	V-2031	1	0.00	6.73	0.00	2
7	V-3377	1	0.00	1.00	0.00	1
9	V-2028	1	0.00	4.39	11.05	1
30	V-7366	2	0.00	2.60	0.20	3
32	V-3449	3	0.00	1.12	0.75	3
36	V-7302	3	0.00	0.05	0.08	1
33	V-7345	3	0.00	0.45	0.80	3
33	V-3038	3	0.00	0.15	2.00	3
33	V-3040	3	0.00	0.01	3.00	3
35	V-7334	3	0.00	0.00	1.50	3
36	V-7302	3	0.00	0.05	0.00	3
36	V-7269	3	0.00	0.17	0.00	3
38	V-7255	3	0.00	0.36	2.00	3
39	V-7229	3	0.00	0.12	3.00	3
40	V-7228	3	0.00	0.04	3.00	3
41	V-7217	3	0.00	0.35	0.60	3
42	V-7295	3	0.00	0.10	2.00	3
43	V-7230	3	0.00	0.03	0.75	3
45	V-7338	3	0.00	0.08	3.00	3
46	V-7225	3	0.00	0.04	0.50	3
47	V-7363	3	0.00	0.16	3.00	3
48	V-7365	3	0.00	0.05	0.75	3
49	V-7432	3	0.00	0.14	2.00	3
50	V-7241	3	0.00	0.35	4.00	3
53	V-7367	4	0.00	9.00	0.05	3
54	V-7291	4	0.00	15.00	0.00	3
57	V-7311	4	0.00	7.50	0.11	3
58	V-7244	4	0.00	5.10	0.09	3
59	V-7220	4	0.00	5.10	0.25	3
60	V-7242	4	0.00	12.50	0.15	3
65	V-7313	4	0.00	12.50	0.10	3
66	V-7266	4	0.00	1.00	0.10	3
69	V-7254	4	0.00	7.50	0.25	3
70	V-3057	4	0.00	14.38	0.40	3
84	V-7093	4	0.00	7.40	0.13	2
100	V-7261	5	0.00	5.00	0.25	2
100	V-7260	5	0.00	7.50	0.03	3
100	V-7430	5	0.00	5.00	0.30	3
100	V-7268	5	0.00	6.80	0.04	3
101	V-7287	5	0.00	3.00	0.10	3
130	V-7105	5	0.00	2.70	0.00	3
130	V-7200	5	0.00	2.50	0.13	2
131	V-3555	5	0.00	10.50	0.00	2
95	V-7315	5	0.00	5.63	0.00	2
155	V-7026	6	0.00	1.98	0.47	2
200	72.2.448	7B	0.00	20.99	0.00	2
127	V-7194	5	0.00	20.01	0.00	1
203	V-7022	7B	0.00	5.90	0.12	2
218	V-7074	8A	0.00	6.20	0.50	2
218	V-7075	8A	0.00	3.80	0.58	2
219	V-7045	8A	0.00	10.40	0.70	2
224	V-7015	8A	0.00	0.42	0.01	2
223	V-7008	8A	0.00	8.26	0.20	2
225	V-7011	8A	0.00	1.60	0.01	2
224	V-7115	8A	0.00	0.60	0.00	2
231	V-7009	8A	0.00	10.40	0.42	2
232	V-7005	8A	0.00	0.29	0.11	2
233	V-7000	8A	0.00	0.46	0.00	2
246	V-3032	8B	0.00	0.82	3.07	2
240	V-7021	8B	0.00	5.00	0.36	2
237	V-7025	8B	0.00	6.07	0.00	2
243	V-7013	8B	0.00	4.04	0.36	2
250	V-7050	9	0.00	7.19	0.66	2
249	V-7198	9	0.00	0.40	0.51	2
257	V-3475	10	0.00	3.10	0.07	2
F10	V-7012	App 3	0.00	0.20	0.00	2
F20	V-7016	App 3	0.00	6.00	0.00	2
F31	V-7014	App 3	0.00	6.74	0.00	2
F34	V-7018	App 3	0.00	1.97	0.00	2

Table 5. Lead isotope ratios.

Acc No	Collection	LRN[1]	Pb 208/206	Pb 207/206	Pb 204/206
V-7015	Sackler	2094	2.7178	0.8821	0.05693
V-7107	Sackler	2150	2.1004	0.8476	0.05412
V-7155	Sackler	2151	2.1326	0.8663	0.05544
FGAV53.92c	Calon da	2152	2.1760	0.8832	0.05681

1. Lab Record Number, Department of Conservation & Scientific Research, FGA/AMSG

Fig. 1. Histogram of zinc content in authentic bronzes from the Eurasian steppes.

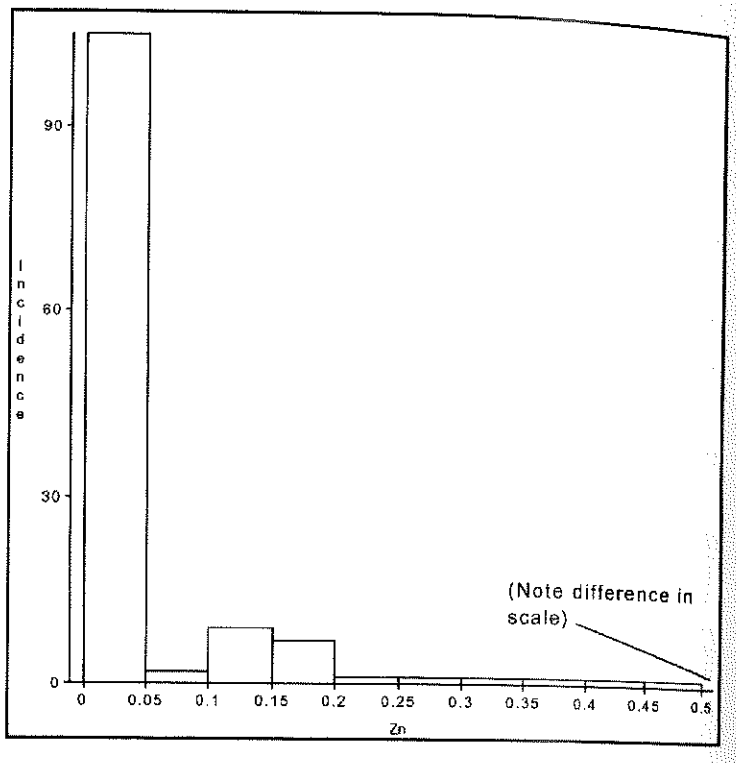

Fig. 2. Histogram of zinc content in forgeries of bronzes from the Eurasian steppes.

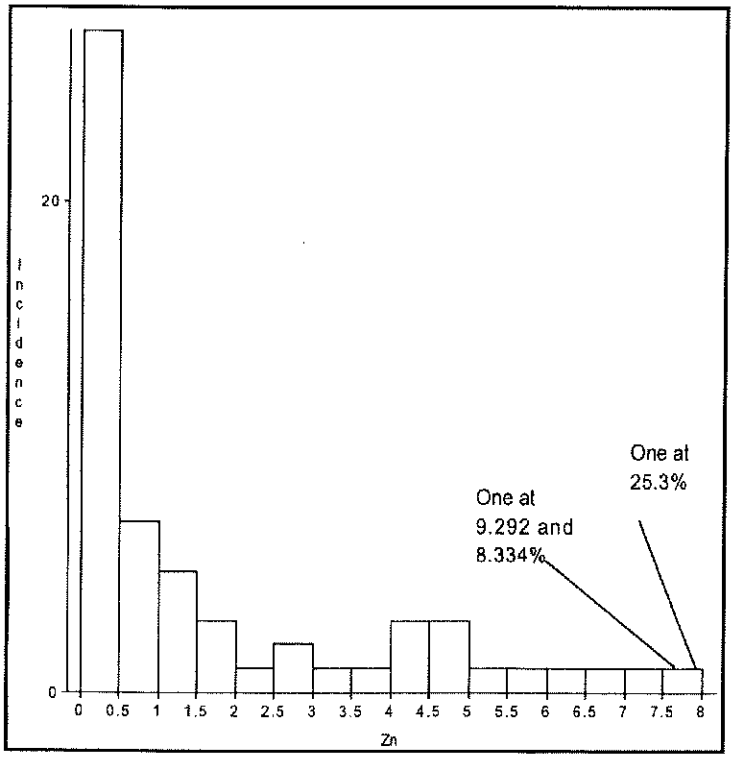

Fig. 3. Histogram of lead content in authentic bronzes from the Eurasian steppes.

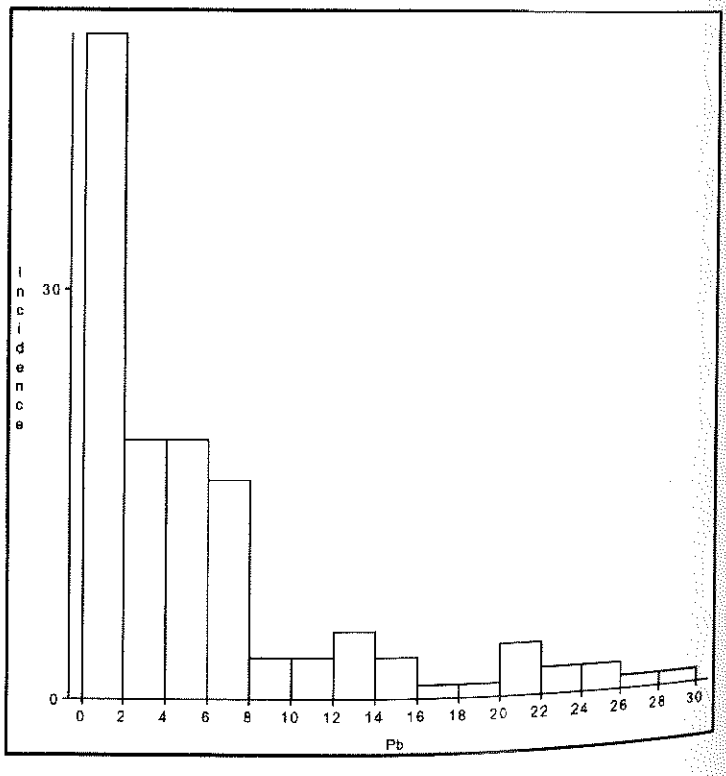

g. 4. Histogram of lead vs. tin in forgeries of bronzes from the Eurasian steppes.

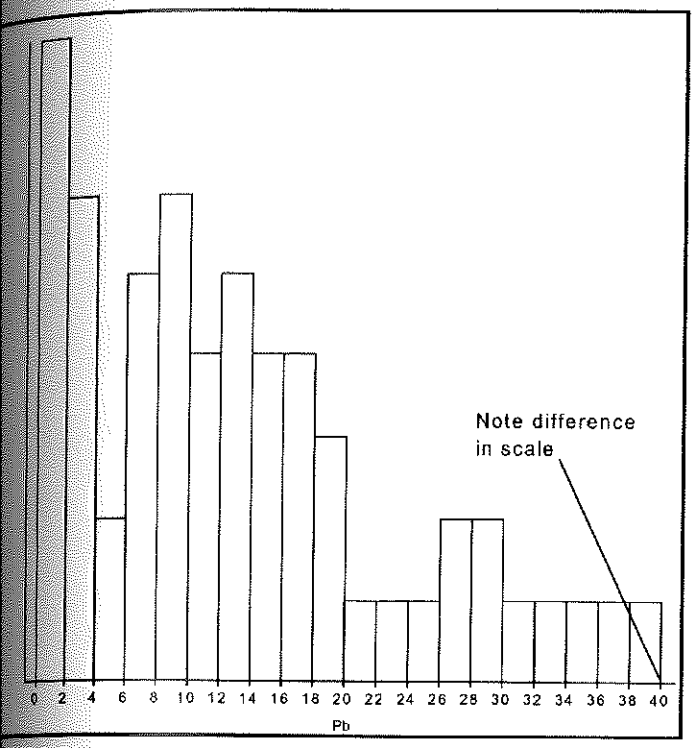

Fig. 5. Plot of lead vs. tin in authentic bronzes from the Eurasian steppes.

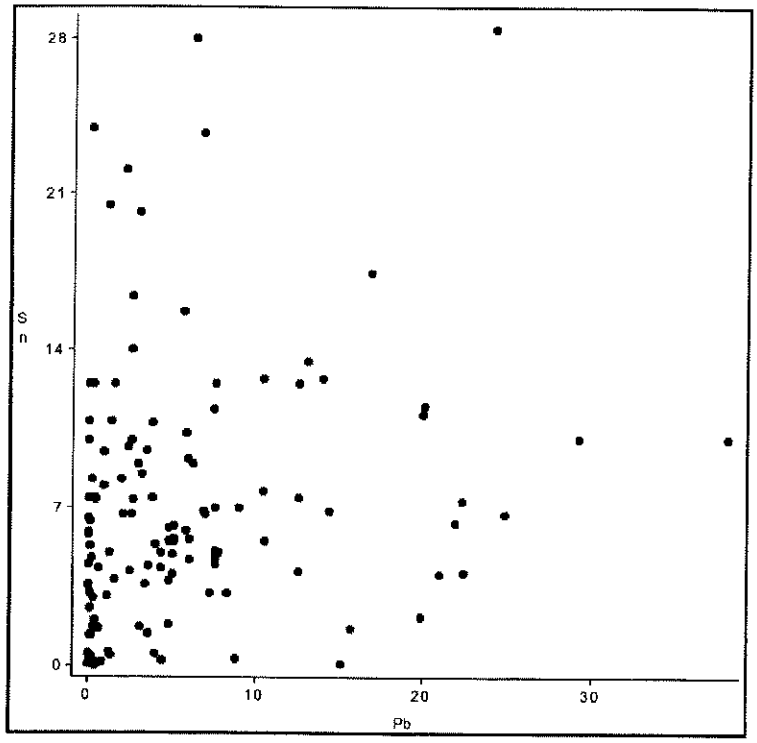

g. 6. Plot of lead vs. tin in authentic bronzes and forgeries of bronzes from the Eurasian steppes. Authentic bronzes are shown in small circles and forgeries in larger squares.

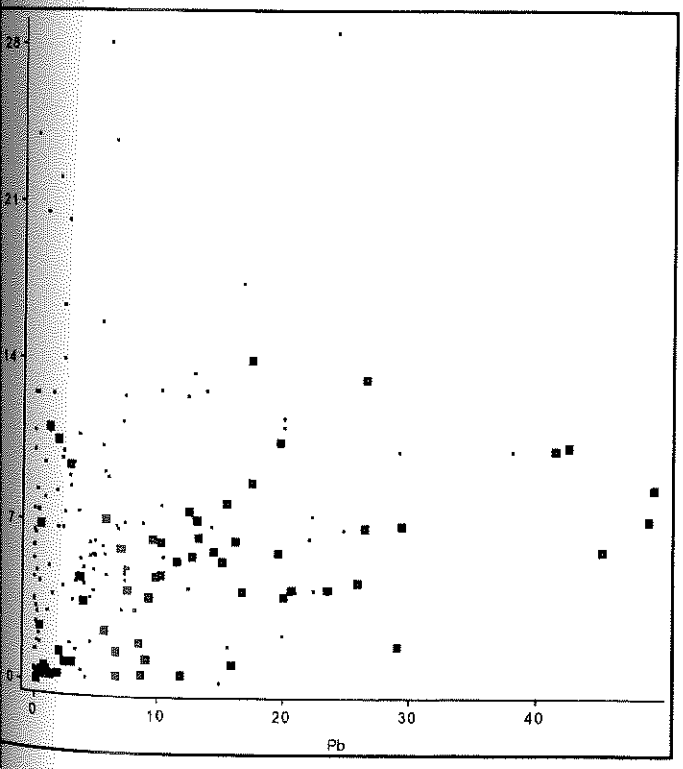

Fig. 7. Plot of lead vs. copper on authentic and forgeries of bronzes from the Eurasian steppes. Authentic bronzes are shown in small circles and forgeries are shown in larger squares.

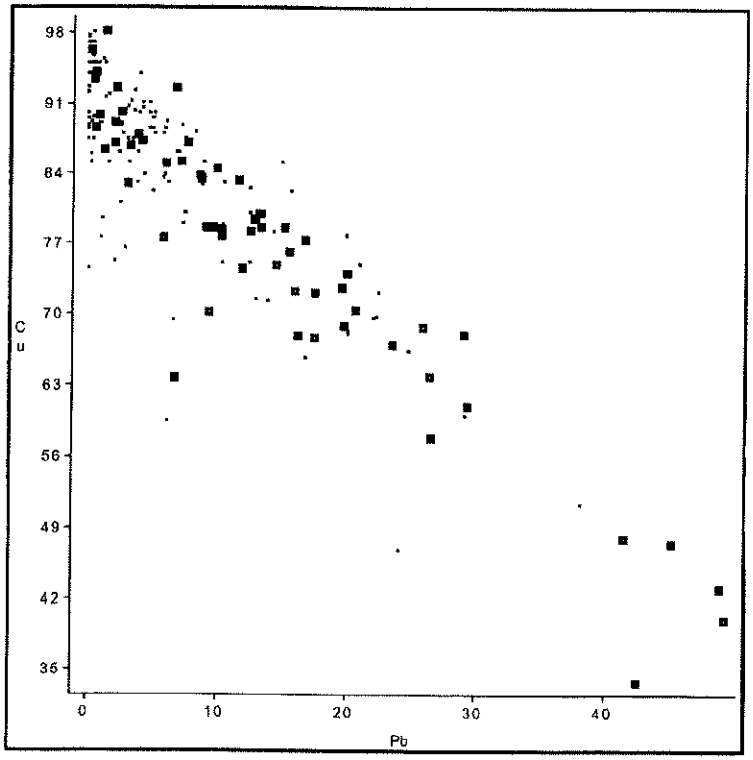

Fig. 8. Plot of tin vs. copper in authentic bronzes and forgeries of bronzes from the Eurasian steppes. Authentic bronzes are shown by solid squares, forgeries by open squares.

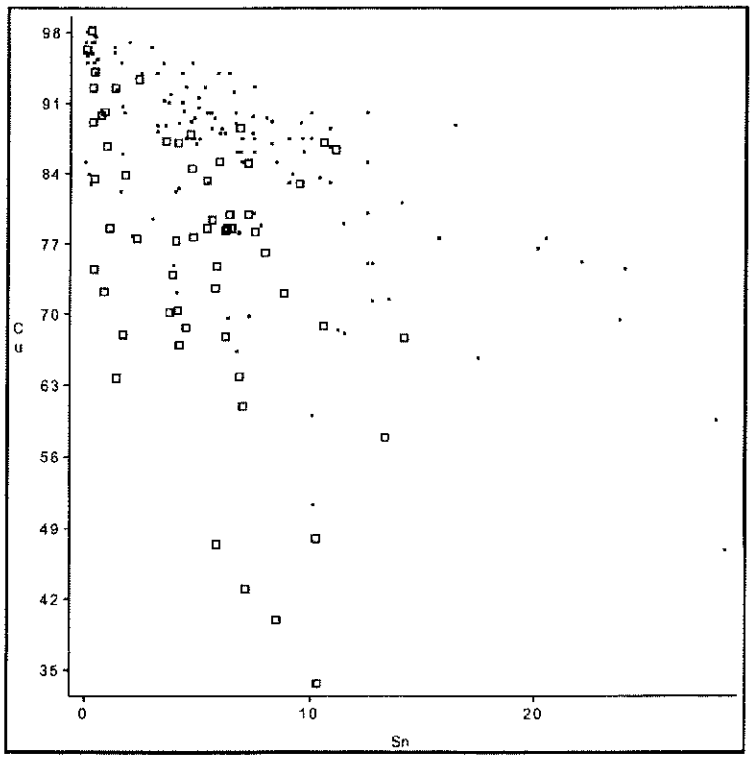

Fig. 9. Lead isotope ratios in four bronzes from the Eurasian steppes compared with other isotope ratio groups.